International Electrical Engineering Journal (IEEJ)
Vol. 5 (2014) No.12, pp. 1680-1687
ISSN 2078-2365
http://www.ieejournal.com/

Control Strategy of Switched Reluctance Motor using Arduino Uno Board

Samia M. Mahmoud[1], Maged N. F. Nashed[2] , Mohsen Z. El-Sherif [3] and Emad S. Abdel-Aliem[4]
[1,3,4]Shoubra Faculty of Engineering, Benha University, Cairo, Egypt
[2]Electronics Research Institute, Cairo, Egypt

[4]emad.sami@feng.bu.edu.eg

***Abstract*—The drive system of switched reluctance motors (SRMs) has a great much attention over the past few years because of the developments of power electronics hardware. Although the SRM is a type of motor that not fed directly through AC or DC source; it uses DC-DC converter between the SRM and DC source. This paper presents drive system of SRM with asymmetric H-bridge converter. The experimental results using Arduino Uno control board under different operating conditions have been presented. The system of SRM is modeled using the MATLAB/SIMULINK software package. Comparison between experimental and simulation results are presented. The experimental results are match and agree with the simulation results.**

***Index Terms*— SRM, Arduino Uno, Asymmetric H-Bridge converter.**

I. Introduction

The SRM represents one of the oldest electric motors. The earliest mention of these motors was established as early in 1838 by Davidson to propel a locomotive in Scotland. However, the full potential of the motor could not be utilized with the mechanical switches available in these days. So, these motors were not widely used in industrial applications due to no simultaneous progress in the field of power electronics and semiconductor switches which are necessary in motor drive. By the end of sixties of the 20th century with the revolution in power electronics, semiconductor switches, microcontrollers, and integrated circuits; the re-invention of these motors is returned by Nasar in his paper in the IEE proceedings in 1969, using the term of "switched reluctance motors" [1,2].

The operation principle is based on the difference in magnetic reluctance for magnetic field lines between aligned and unaligned rotor positions. When a stator coil is excited, the rotor experiences a force which will pull the rotor to the aligned position because the reluctance of the magnetic path is minimized. The aligned position of a phase is defined to be the situation when the stator and rotor poles of the phase are perfectly aligned (fully overlapped produces zero torque in this period) with each other attaining the minimum reluctance position, *i.e* the stator excited flux becomes maximum. The phase inductance is maximum (L_a) in this position. The phase inductance decreases gradually as the rotor poles move away from the aligned position in either direction. When the rotor poles are symmetrically misaligned with the stator poles of a phase, the position is said to be the unaligned position. The phase has the minimum inductance (L_u) in this position [3].

The principle of operation depends on switching of currents into stator windings sequentially and only the sequence of excitation of stator phases determines the direction in which the rotor will rotate. To achieve continuous rotation, the stator phase currents are switched 'on' and 'off' in each phase in a sequence manner. The successive movement of three phases, 6/4 SRM is shown in Fig. 1. The synchronization of the stator phase excitation is readily accomplished with rotor position feedback [4,5].

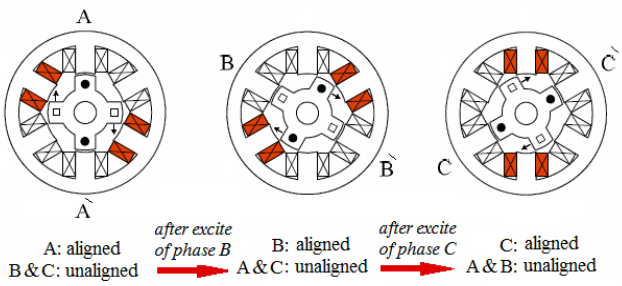

Fig. 1 Successive phase energizing of 3-ph, 6/4 SRM

According to the movement of SRM shown in Fig. 1, the shaft will turn a precise distance when a pulse is receive from the power converter. The SRM has a stator consists of six poles and rotor consists of four poles. The motor will move 12 steps for making one complete revolution. This means that the rotor has 12 possible detent positions. When the rotor is in a detent position, it will have enough magnetic force to keep the shaft from moving to the next position. By changing the current flow to the next stator winding, the rotor will only move one step of 30°. When a constant current is passed through one phase, the motor generate a torque. This torque is typically a sinusoidal function of rotor displacement from the detent position. When the stator and rotor teeth are fully aligned, the circuit reluctance is minimized and the magnetic flux is at its maximum value.

www.ieejournal.com/

International Electrical Engineering Journal (IEEJ)
Vol. 5 (2014) No.12, pp. 1680-1687
ISSN 2078-2365
http://www.ieejournal.com/

II. Dynamic Modeling Of SRM

The SRM is always operated in the magnetically saturated mode to maximize the energy transfer. The magnetic flux linked by a single phase must be known to produce the developed torque. The high degree of SRM nonlinearity makes it impossible to model the flux linkage or phase inductance exactly. The highly nonlinear nature of the SRM makes the linear model unsuitable for high performance applications. Therefore, various methods have been applied to adapt the parameters, especially the inductance, to the operating conditions, accounting for the nonlinear characteristics of the magnetic field. In an alternative approach, the flux linkage is selected directly as the variable instead of treating the flux linkage as the product of inductance and current. In a SRM, the phase inductances and flux linkages vary with rotor position due to the saliency of stator and rotor poles. The selection of a SRM model from the existing two models, inductance model or flux linkage model, depends on a proper mathematical representation of the static characteristics, and on the computational facilities and control techniques available.

An important step in any control system design is to develop a good mathematical model, which represents the plant under various operating conditions. The complete dynamic mathematical model of the SRM in [6,7] is a set of differential equations, which are obtained using standard electromagnetic theory. These differential equations are as follows:

First; the electrical state equations of the SRM can be expressed as:

$$U_j = i_j R_j + \frac{d\lambda(i_j,\theta)}{d\theta} \tag{1}$$

Where U_j is the phase voltage, i_j is the phase current, R_j is the phase resistance, j is the active phase, $\lambda_j(i_j,\theta)$ is the flux linkage, and θ is the rotor position. Eqn. (1) can be rewritten as:

$$U_j = i_j R_j + \frac{\partial\lambda(i_j,\theta)}{\partial i}\frac{di_j}{dt} + \frac{\partial\lambda(i_j,\theta)}{\partial\theta}\frac{d\theta}{dt} \tag{2}$$

The flux linkage in an active phase is given by the product of the self-inductance and the instantaneous phase current as follows:

$$\lambda(i_j,\theta) = L_j(i_j,\theta)\cdot i_j \tag{3}$$

Substituting Eqn. (3) into Eqn. (2) gives:

$$U_j = i_j R_j + L_{jinc}\cdot\frac{di_j}{dt} + i_j\cdot\frac{\partial L_j(i_j,\theta)}{\partial\theta}\cdot\omega \tag{4}$$

$$= i_j R_j + L_{jinc}\cdot\frac{di_j}{dt} + K_v\cdot\omega \tag{5}$$

$$L_{jinc} = \frac{\partial\lambda_j(i_j,\theta)}{\partial i} = \frac{(\partial L_j(i_j,\theta)\cdot i_j)}{\partial i} = L_j(i_j,\theta) + i_j\cdot\frac{\partial L_j(i_j,\theta)}{\partial i} \tag{6}$$

$$\omega = \frac{d\theta}{dt} \tag{7}$$

Where L_{jinc} is the phase incremental inductance, K_v is the current-dependent back-emf coefficient, and ω is the rotor angular speed.

Rearranging Eqn. (4) gives:

$$\frac{di_j}{dt} = \frac{1}{L_{jinc}}\left(U_j - i_j R_j - i_j\cdot\frac{\partial L_j(i_j,\theta)}{\partial\theta}\cdot\omega\right) \tag{8}$$

Second; the mechanical state equation of the SRM can be expressed as follows:

$$J\frac{d^2\theta}{dt^2} = J\frac{d\omega}{dt} = \sum_{J=1}^{N_{ph}} T(i_j,\theta) - B\omega - T_L(\omega) \tag{9}$$

Where J and B are the moment of inertia and the viscous friction coefficient, respectively; and T_L is the load torque. Eqns. (7), (8) and (9) represent the complete mathematical model of the SRM.

III. Description Of The System For SRM

The 3-ph SRM that used is designed, constructed, and assembled in the laboratory of Electronics Research Institute in Cairo and the other parts of the drive system are built and tested in the electrical machines laboratory at Shoubra Faculty of Engineering. An experimental block diagram of the SRM system is shown in Fig. 2. A photograph of the experimental setup contains all parts of the drive system is shown in Fig. 3.

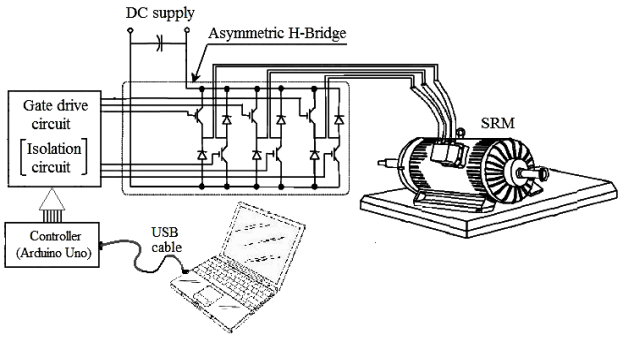

Fig. 2 An experimental block diagram of 3-ph SRM drive system

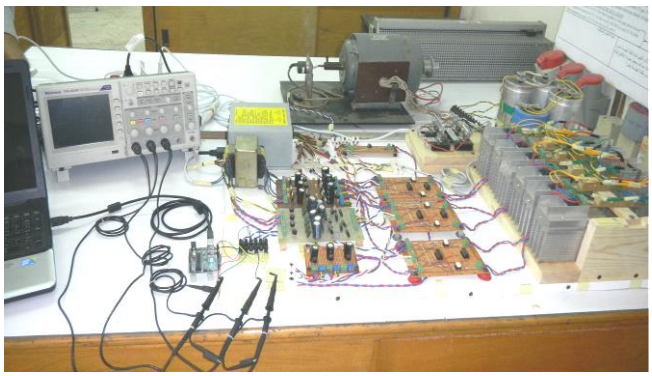

Fig. 3 A photograph of the experimental setup

www.ieejournal.com/

International Electrical Engineering Journal (IEEJ)
Vol. 5 (2014) No.12, pp. 1680-1687
ISSN 2078-2365
http://www.ieejournal.com/

The setup drive system consists of two main parts, the software part and the hardware part. The hardware parts are shown in Fig. 2 but the software part is the Arduino software that used for written the control program of the drive system. This control program can be loaded in the Arduino Uno board to drive the SRM system.

The hardware consists of main five parts which are a three phase 6/4 SRM, asymmetric H-bridge converter, gate drive circuit, controller, and DC power supplies. The motor that used in the simulation results in the same motor that is used in the experimental setup, its parameters is presented in Appendix. All hardware components will be described in details the next subsections.

The schematic diagram of the 3-ph 6/4 SRM is shown in Fig. 4. All dimensions in *mm*. A photograph of it is shown in Fig. 5.

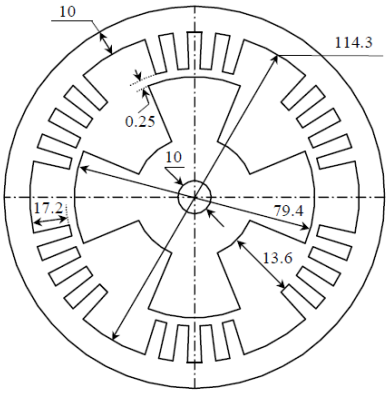

Fig. 4 The geometrical shape for the stator and rotor together

Fig. 5 A photograph of the 3-ph 6/4 SRM

The SRM can not run directly from DC or AC supply. So, DC-DC converter must be connected between the DC supply and the SRM. Inside the converter; the operation of the motor must be commutated to feed the supply voltage for the phase's windings of the motor. So, the asymmetric H-bridge converter is used in the experimental setup here. The power circuit of the H-bridge converter is shown in Fig. 6 and a photograph of the converter is shown in Fig. 7.

As appeared in Fig. 7; the upper row consists of six power switches IGBT of type *IRG4PF50WD*, they chosen due to its high voltage rating, high current rating, and fast turn on-off speed. The lower row consists of six fast recovery freewheeling diodes of type *12FL10-S02*. Each switch or diode is mounted on a heat sink for cooling. The switches and diodes in the bridge are supported with protective snubber circuits; as shown in Fig. 8, to eliminate and absorb the switching voltage spikes which are results from the accumulating switching off of power switches and motor phase inductances. Each switch or diode has *RC* snubber circuit. The values of the snubber circuit components are $R_T = R_D = 15\Omega$, $C_T = 12\mu F$, and $C_D = 10\mu F$.

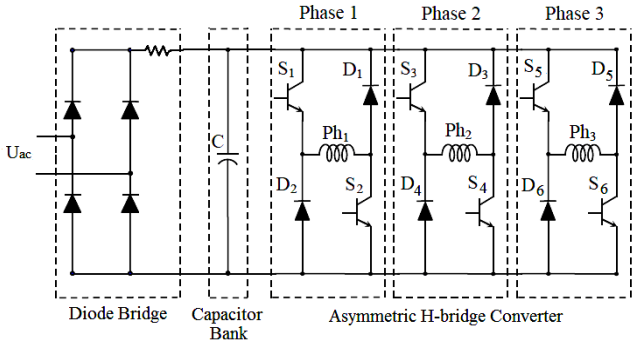

Fig. 6 A symmetric H-bridge converter connected to AC supply through diode bridge and capacitor bank

Fig. 7 A photograph of asymmetric H-bridge converter

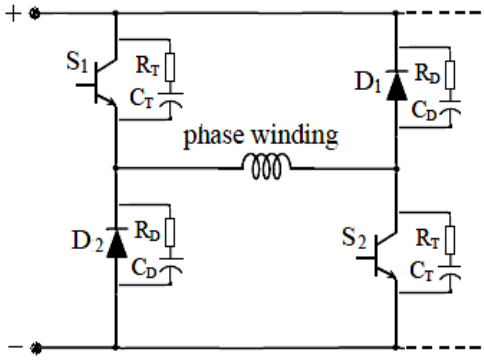

Fig. 8 One phase of H-bridge converter with snubber circuits

The gate drive circuit is located between the controller and the power H-bridge converter. The control logic signals or the switching signals that comes from the controller are too small to drive the power switches of H-bridge converter. So, the gate drive circuit is used for two reasons: the first

International Electrical Engineering Journal (IEEJ)
Vol. 5 (2014) No.12, pp. 1680-1687
ISSN 2078-2365
http://www.ieejournal.com/

one is to amplify the control logic signals to the value of current levels required for switching the power converter, and the second reason is that the drive circuit acts as a good isolation between the controller and the power converter. Fig. 9 shows the components of one phase in the gate drive circuit that needed to drive the gates of the IGBTs in the H-bridge converter.

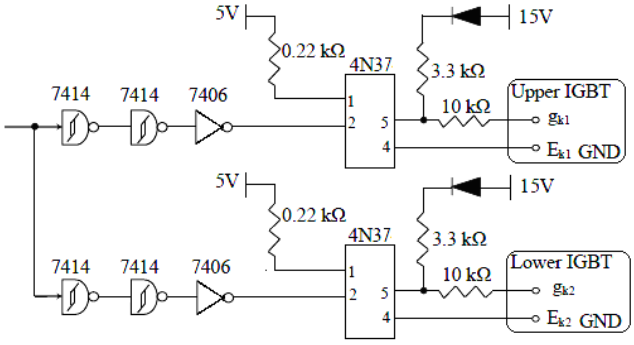

Fig. 9 One phase of the gate drive circuit

In each phase, the logic signal coming from the controller is split into two symmetrical signals. Each signal is passed through two Schmitt trigger inverter SN74LS14 and then is followed by one NOT gate of an open-collector buffer circuit SL74LS06 for boosting the current signal. The opto-coupler 4N37 receives signal of +5V and sends signals of +15V. The output of each opto-coupler is connected across the gate and emitter of IGBT, where the emitter terminal is connected to its gate driver ground. A photograph of the three phase gate drive circuit is shown in Fig. 10. Note, the GND terminal of source 5V is connected to the GND pin of the controller.

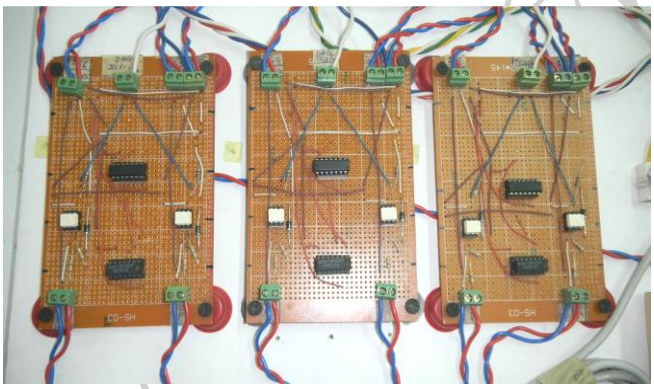

Fig. 10 A photograph of the three phase gate drive circuit

The interfacing system hardware needs controller. The controller may be a data acquisition card, but it has a high price, so in our work we will use a controller named Arduino Uno board that has a low price. The Arduino Uno is a microcontroller board based on the ATmega328. It has 14 digital I/O pins (of which 6 can be used as PWM outputs), 6 analog inputs, 16 MHz ceramic resonator, a power jack, a USB connection, and a reset button. To support the board with electric power, a USB cable connected between the computer and the Arduino board, or using USB adapter between the AC source and the Arduino board. A photograph of the board with USB cable is shown in Fig. 11.

Fig. 11 A photograph of Arduino board with a USB cable

To write the program for controlling the experimental hardware, we must use the Arduino software. The program after be written can be uploaded to the Arduino board for generating the control logic signals required to run the motor depending on the rotor position. The Arduino Uno can be communicated another Arduino, or other microcontrollers.

The dc power source for H-bridge is shown in Fig. 6. This power source consists of Diode Bridge that has four diode of type *BYX52-600* and four large DC electrolytic capacitors of type *FELSIC-039* (4x1650µF, 1000V). These capacitors are connected across the power source to hold a very low power returned form the motor to the supply. A photograph of DC source for H-bridge is shown in Fig. 12.

A step down AC voltage transformer (220/16/6V), having 16 terminals, is used to feed all separate dc power sources. The output ac voltage of the transform is rectified through a diode rectifier bridge and then fed to a dc voltage regulator.

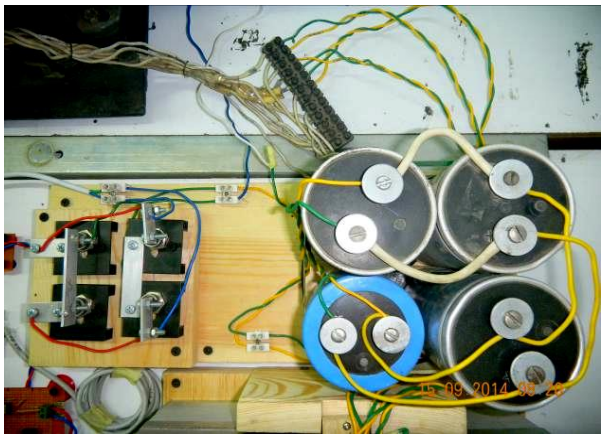

Fig. 12 A photograph of DC power source for H-bridge converter

A photograph of the circuits used to produce DC voltage of +5V and +15V is appeared in Fig. 13. Also, the transformer that used to produce a DC voltage of +15V must have isolated windings.

International Electrical Engineering Journal (IEEJ)
Vol. 5 (2014) No.12, pp. 1680-1687
ISSN 2078-2365
http://www.ieejournal.com/

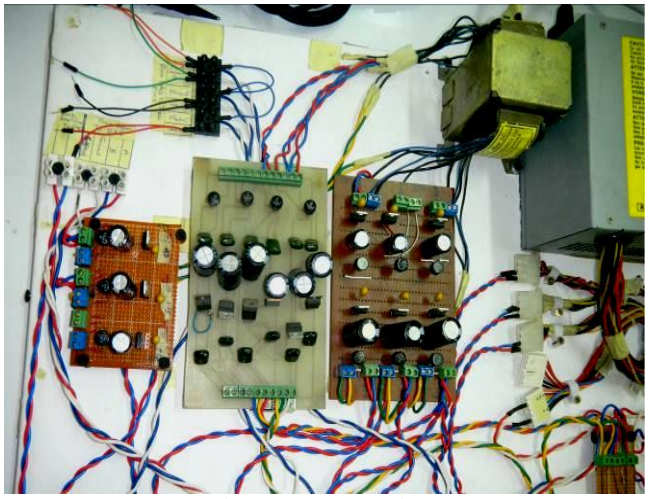

Fig. 13 A photograph of DC power sources for ICs in gate drive circuit

IV. Experimental Results

Comparison between experimental and simulation results are presented in this section using the prototype that explained in details in the previous sections. The experimental results of SRM system are compared with the simulation results at low, medium, and rated speed.

A- Results for low speed

If the motor be wanted to rotate at low speed, the output pulses of the Arduino board that send to the three phases of the motor are shown in Fig. 14 (a). For each phase, during one cycle, the turn-on time equals 62mSec. The output pulses of the Arduino have a value of +5V. The simulation results that corresponding to the experimental results is shown in Fig. 14 (b). Theses results show that there is no overlap between the motor phases.

The voltage signal across one phase for the motor at low speed is shown in Fig. 15. In Fig. 15 (a), the experimental result, the waveform has very low spikes due to the turn off of the switches in the converter. The supply voltage across the phase is +26V during turn-on of the phase and -26V during turn-off of the phase.

The experimental waveform for the current in one phase is shown in Fig. 16 (a). The maximum value of the phase current is about 1.05A. But the maximum value of the current in the simulation results in Fig. 16 (b) is maximum 1.2 A. The current in experimental is match with simulation. However, there is small error in the value because there is losses appears in the drive circuit not be considered in the Simulink model.

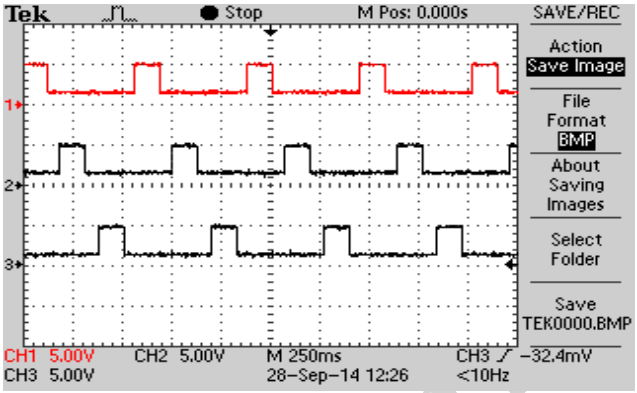

(a) Experimental result

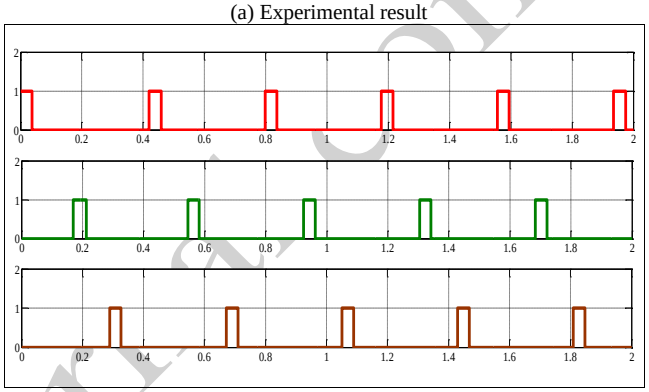

(b) Simulation result

Fig. 14 Output of controller at low speed

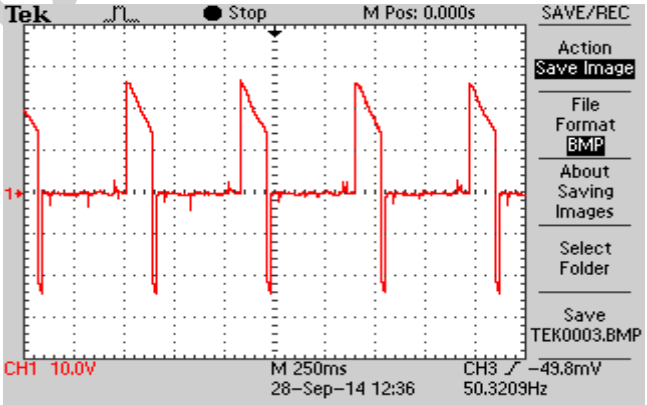

(a) Experimental result

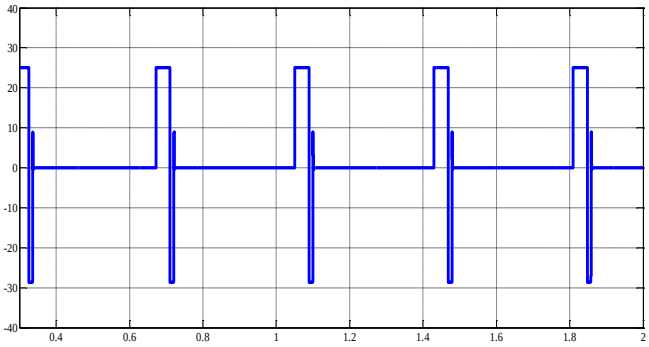

(b) Simulation result

Fig. 15 Voltage waveform of one phase at low speed

International Electrical Engineering Journal (IEEJ)
Vol. 5 (2014) No.12, pp. 1680-1687
ISSN 2078-2365
http://www.ieejournal.com/

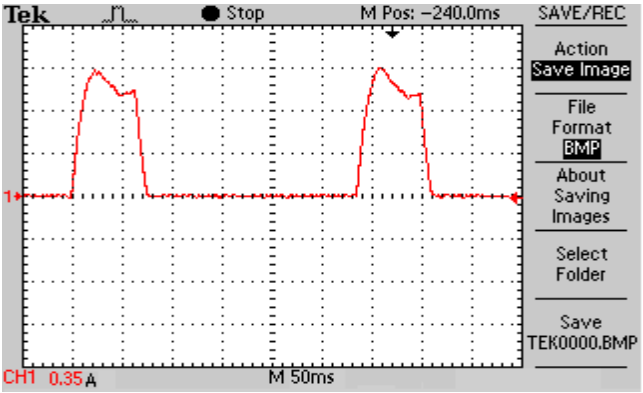

(a) Experimental result

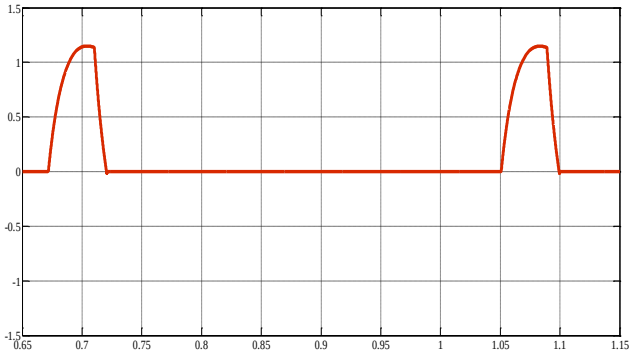

(b) Simulation result

Fig. 16 Current waveform of one phase at low speed

B- Results for medium speed

If the motor be wanted to rotate at medium speed, the output pulses of the Arduino board that send to the three phases of the motor are shown in Fig. 17 (a). For each phase, during one cycle, the turn-on time equals 10mSec.

Note that, the turn-on time in this speed is smaller than the turn-on time in low speed. This means that, if be wanted to increase the motor speed. The frequency must be increase and the turn-on time decreased.

The voltage signal across one phase for the motor at medium speed is shown in Fig. 18. In Fig. 18 (a), the experimental result, the waveform has high spikes due to turning-off of the switches in the converter that occurs at high voltage of 265V. The supply voltage across the phase is +265V during turn-on of the phase and -265V during turn-off of the phase. The negative part of the voltage not appears in experimental result because the maximum limit of the oscilloscope screen.

The experimental waveform for the current in one phase is shown in Fig. 19 (a). The maximum value of the phase current is about 2.75A. While, the current in the simulation results in Fig. 19 (b) is about 3A. The current in simulation result is greater than the current in experimental because there is losses appears in the drive circuit not be considered in the Simulink model.

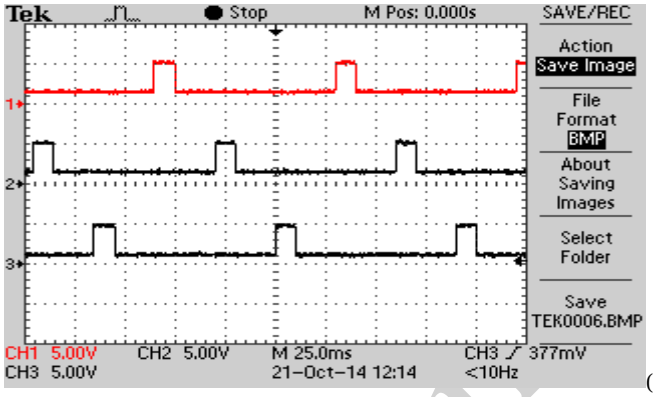

a) Experimental result

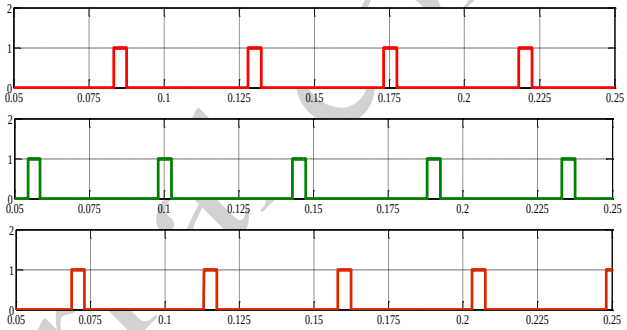

(b) Simulation result

Fig. 17 Output of controller at medium speed

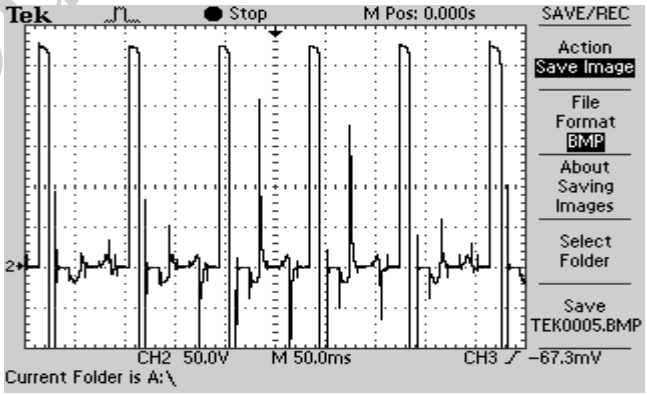

(a) Experimental result

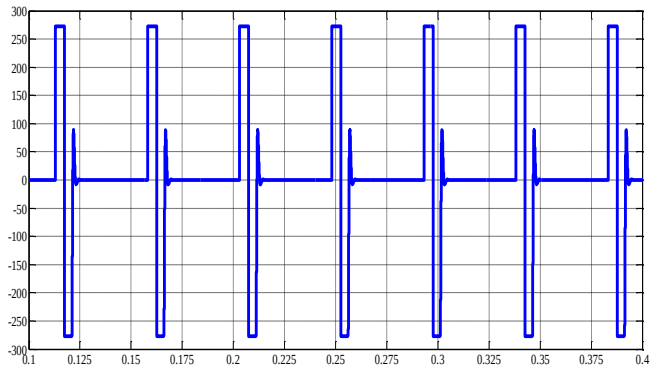

(b) Simulation result

Fig. 18 Voltage waveform of one phase at medium speed

International Electrical Engineering Journal (IEEJ)
Vol. 5 (2014) No.12, pp. 1680-1687
ISSN 2078-2365
http://www.ieejournal.com/

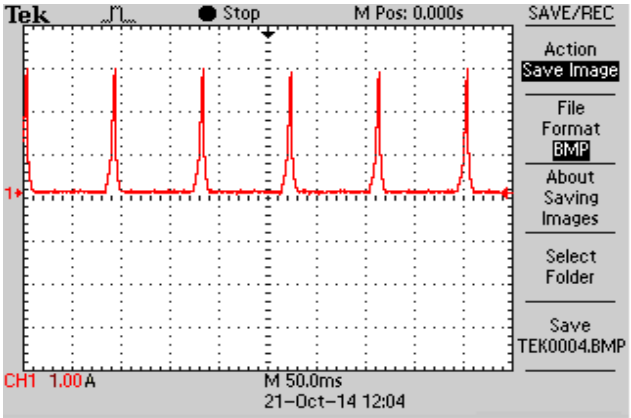

(a) Experimental result

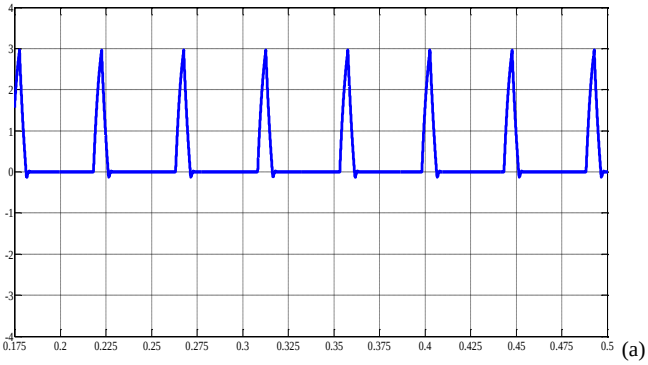

(b) Simulation result

Fig. 19 Current waveform of one phase at medium speed

The speed waveform can be measured using position sensor, *RS stock no.341-581*, the signal of the speed is measured as digital signal. In Fig. 20, the digital speed of SRM is starting and the time of pulses is decreased.

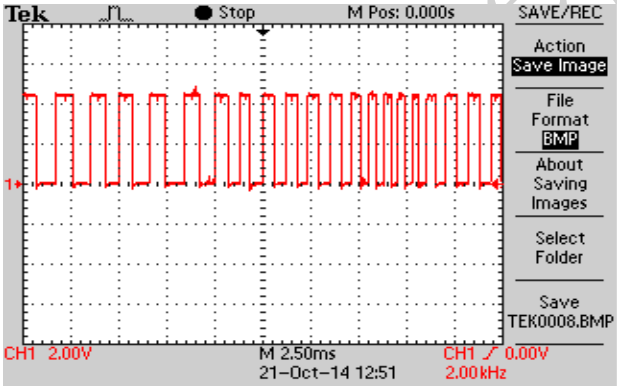

Fig. 20 The Experimental result of digital speed waveform

C- Results for rated speed

For rotation of the motor at rated speed, the output pulses of the Arduino Uno board that send to the three phases of the motor are shown in Fig. 21 (a). Theses results show that there is no overlap between the motor phases, In other words, there is no delay time between any phase and the next one. The sequence of pulses for simulation results for rated speed is shown in Fig. 21 (b).

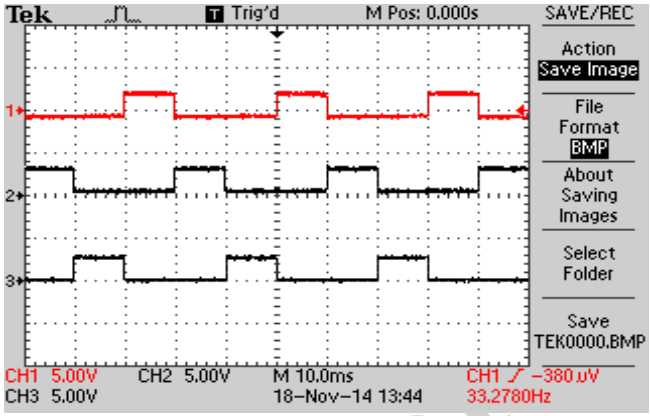

(a) Experimental result

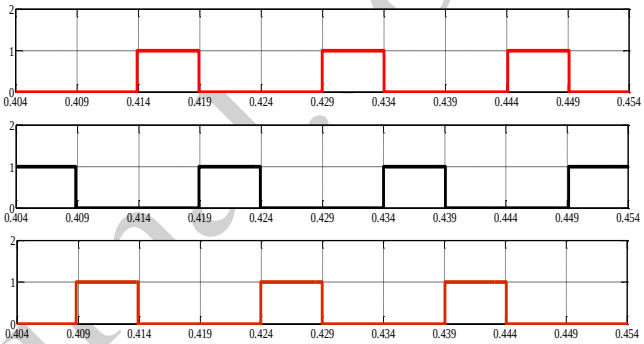

(b) Simulation result

Fig. 21 Output of controller at rated speed

The experimental and simulation result for waveform of voltage across one phase at rated speed are shown in Fig. 22 (a) and Fig. 22 (b) respectively. The voltage signal has positive value when the current is increased in the phase, but, it has a negative value when the current is decreased in the phase. The spikes in the voltage signal across the phase are due to the turning-off of the switch in the power converter.

The experimental and simulation result for current waveform in one phase at rated speed are shown in Fig. 23 (a) and Fig. 23 (b) respectively. The current signal has a spike shape because the time of passing current is very low, i.e., as the turn-on time of power switches decreases then the speed increases and also the phase current takes the shape of spikes.

International Electrical Engineering Journal (IEEJ)
Vol. 5 (2014) No.12, pp. 1680-1687
ISSN 2078-2365
http://www.ieejournal.com/

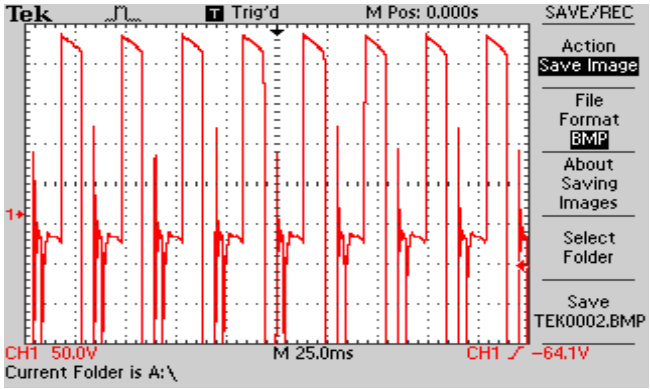

(a) Experimental result

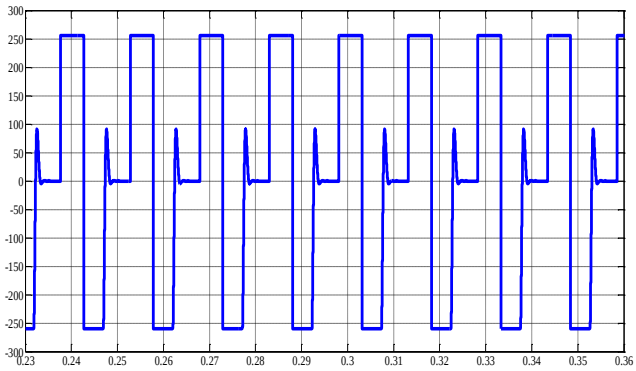

(b) Simulation result

Fig. 22 Voltage signal across one phase at rated speed

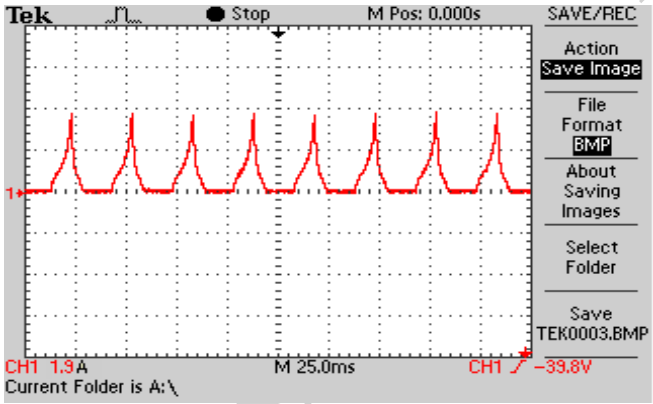

(a) Experimental result

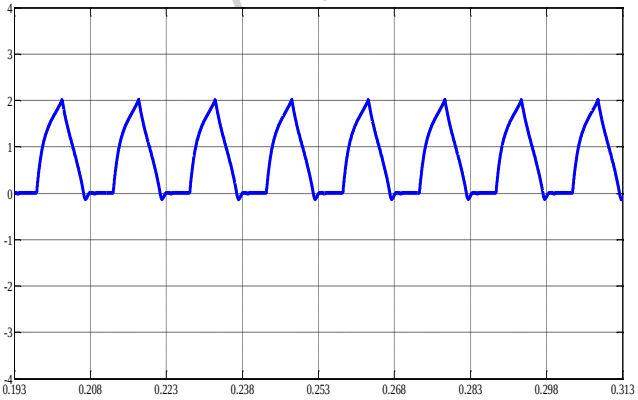

(b) Simulation result

Fig. 23 Current signal of one phase at rated speed

V. Conclusion

Asymmetric H-bridge converter are one of the converters in SRM control. The system of 3-phases SRM with control was presented. The experimental and simulation results are compared at low, medium, and rated speed.

Control of SRM is expensive, the paper introduces the control with simple cost using Arduino controller. The experimantal system is fast and stable. Variable speed of system are providing operational and flexibility. The experimental results are matched and agreed with the simulation results.

Appendix

Table I Switched Reluctance Motor Parameters

Number of motor phases	3	Rated speed	1000rpm
Number of stator poles	6	Rated phase current	3A
Number of rotor poles	4	Rated torque	1Nm
Stator pole arc (mech. deg)	40º	Number of turns per phase	600
Rotor pole arc (mech. deg)	45º	Winding wire diameter	0.5mm
DC voltage rating	220V	Rotor pole arc (mech. deg)	30º
Stator phase resistance	17Ω	Inertia constant	0.0013 Kg.m^2
Aligned inductance	0.605 H	Viscous friction coefficient	0.0183 N.m.Sec^2
Unaligned inductance	0.155 H		

Acknowledgements

Many thanks to the professors and colleagues in Electrical Engineering Department, Benha University and the team of Electronics Research Institute for helpful and encouragement.

References

[1] S. A. Nasar, "Electromagnetic Energy Conversion Devices and Systems," Englewood Cliffs, Prentice-Hall, 1970, (Book).

[2] S. A. Nasar, "DC Switched Reluctance Motor," Proceedings of the Institution of Electrical Engineers, Vol.166, No. 6, June, 1969, pp.1048-1049.

[3] Khaldoon Asghar, "Analysis of Switched Reluctance Motor Drives for Reduced Torque Ripple using FPGA based Simulation Technique" American Journal of Information Sciences, Vol. 6, No. 2, 2013

[4] Mukhtar Ahmad, "High Performance AC Drives: Modelling Analysis and Control," Springer Press 2010, (Book), "Chapter 6: Switched Reluctance Motor Drives (SRM)".

[5] Ahmed O. Khalil, "Modeling And Analysis Of Four Quadrant Sensorless Control of A Switched Reluctance Machine Over The Entire Speed Range," PhD Dissertation, The Graduate Faculty of the University of Akron, August 2005.

[6] Timothy L. Skvarenina, "The power electronics handbook," CRC Press, 2002, (Book), "Chapter 13: Switched Reluctance Machines," by Iqbal Husain.

[7] Jin-Woo Ahn, Jianing Liang and Dong-Hee Lee "Classification and Analysis of Switched Reluctance Converters," Journal of Electrical Engineering & Technology Vol. 5, No. 4, pp. 571-579, 2010.